Pathology International

Pathology International 2014; **64**: 209–216 doi:10.1111/pin.12164

Original Article

Optimal fixation for total preanalytic phase evaluation in pathology laboratories. A comprehensive study including immunohistochemistry, DNA, and mRNA assays

Masaaki Sato,[1] Motohiro Kojima,[1] Akiko Kawano Nagatsuma,[1] Yuka Nakamura,[1] Norio Saito[2] and Atsushi Ochiai[1]

[1]*Division of Pathology, Research Center for Innovative Oncology, National Cancer Center,* [2]*Colorectal and Pelvic Surgery Division, National Cancer Center Hospital East, Kashiwa, Chiba, Japan*

The purpose of this study was to set the optimal preanalytical fixation protocol to enhance analytical and postanalytical phase accuracy and consistency. Twenty-five normal colorectal tissues were fixed using various formalin concentrations, pHs, and fixation periods. All specimens were embedded in paraffin and 4 μm sections were used for immunohistochemistry of Ki-67, and extraction and amplification of DNA and RNA. The Ki-67 labeling index and the successful gene amplification rate for DNA and mRNA were evaluated and compared among variously fixed tissue samples. Ki-67 positivity was enhanced by low pH and short fixation time, and was influenced by the type of antibody, but not by the staining (with or without using an autostainer) method. DNA amplification by PCR was strongly influenced by pH of formalin. cDNA amplification could be accomplished only with the shortest PCR fragment of 142 bp, and longer fixation times impaired the amplification. These data suggest that multiple different factors influence immunohistochemical results and gene amplification using DNA and mRNA. We recommend, based on data from this comprehensive analysis, a 10% neutral buffered formalin and fixation times of no longer than 1 week to produce consistent immunohistochemical slides and DNA amplification within 500 bp in pathology laboratories.

Key words: fixation, pathology, preanalytic phase

The numerous components of laboratory test processes can be categorized into preanalytic, analytic, and postanalytic phases. Many laboratory tests using formalin-fixed and paraffin-embedded tissue samples in the preanalytic phase have been developed. Fixation is one of the most important steps in the preanalytic phase in pathological testing. Multiple factors including kinds of fixative, fixation duration, and acidity levels have been reported to have an effect on immunohistochemical results and gene amplification. For these reasons, a standardized and optimized fixation protocol for pathology laboratories would allow for more consistent and accurate data to be produced and enable better informed decisions based on the results.[1–8]

However, the current recommendations for preanalytic phase testing vary depending on what organ, therapy, or procedure (such as protein, DNA, or RNA assay) is being used.[9–18] Furthermore, most studies investigating the effects of fixation in laboratory testing have dealt with only one kind of laboratory test target. A standardized fixation protocol for pathology laboratories should be made available. We analyzed Ki-67 immunohistochemistry (IHC) testing and polymerase chain reaction (PCR)-based gene amplification using DNA and mRNA from one samples that was fixed by different protocols to clarify how variations in fixation influence postanalytic results in different assays. In regards to IHC testing, we also evaluated the effect of staining procedures, autostainer or manual staining, and different antibody clones, to search for the best way to reduce the effect of nonstandardized fixation protocols.

In this study, we performed comprehensive analyses using IHC and PCR procedures on one tissue block to develop an optimized fixation protocol available for use in pathology laboratories to enhance testing accuracy and consistency.

MATERIALS AND METHODS

Sample preparation

Twenty-five cases of the normal colorectal tissue samples 2.0 × 1.0 cm in size were obtained from surgically resected

Correspondence: Atsushi Ochiai, MD, PhD, Research Center for Innovative Oncology, National Cancer Center Hospital East, 6-3-1 Kashiwanoha, Kashiwa, Chiba, 277-8577, Japan. Email: aochiai@east.ncc.go.jp

Received 21 January 2014. Accepted for publication 2 April 2014.

Table 1 Types of fixatives

Fixatives	Buffer	pH value
10% NeuBF		7.5
10% NonBF	non	4.1
10% at pH 4	100 mM citrate	4.1
10% at pH 6	100 mM phosphate	6.1
10% at pH 7	100 mM phosphate	7.0
10% at pH 8	100 mM phosphate	7.9
20% NeuBF		7.5
20% NonBF	non	3.9

10% NeuBF, 10% neutral buffered formalin (Wako); 10% NonBF, 10% formalin; 10% at pH 4, 10% formalin with buffer at pH 4; 10% at pH 6, 10% formalin with buffer at pH 6; 10% at pH 7, 10% formalin with buffer at pH 7; 10% at pH 8, 10% formalin with buffer at pH 8; 20% NeuBF, 20% neutral buffered formalin (Wako); 20% NonBF, 20% formalin.

colorectal cancer cases at the National Cancer Center Hospital East between 2011 and 2012. All obtained tissues were fixed in 100 mL of formalin with various pHs and concentrations within 1 hour after removal from the colon. The eight types of formalin solutions are shown in Table 1. These specimens were fixed for 24 h, 48 h, 1 week, or 2 weeks. All differently fixed tissues were processed using Vacuum Rotary VRX-23 (Sakura Finetek, Tokyo, Japan), and embedded in paraffin. The present study was approved by the local research ethics committee of the National Cancer Center Hospital East (No.21–080).

Immunohistochemistry

The tissue was cut from paraffin blocks in 4 μm sections using a microtome and stretched on a water bath at 43°C, then mounted on glass slides. The slides were incubated at 37°C overnight. Ki-67 staining was performed manually by the standard immunohistochemical method. The slides were deparaffinized in xylene and hydrated in ethanol. Antigen retrieval was performed with 10 mM citrate buffer (pH 6.0) in a microwave oven at 95°C for 20 min. Endogenous peroxidase was blocked by incubation for 15 min with 0.3% hydrogen peroxidase in methanol. Nonspecific binding was blocked by incubating in phosphate-buffered saline (PBS) containing 2% normal swine serum and 0.1% sodium azide for 30 min. The primary antibody was diluted in PBS containing 2% normal swine serum and 0.1% sodium azide. The sections were incubated with mouse anti-human Ki-67 antibody with 1:100 dilutions for 1 h at room temperature. The clone MIB-1 (Dako, Glostrup, Denmark) monoclonal antibody against Ki-67 was used. After the wash with PBS, slides were incubated for 30 min using Dako Envision Labelled Polymer-HRP anti-mouse. The staining was visualized with 3,3′-diaminobenzidine for 4 min and counterstained with Mayer's hematoxylin, dehydrated in ethanol, and cleared in xylene. Other antigen retrieval methods were also performed using Target Retrieval Solution, pH 9 (Dako) or Dako Proteinase K, Ready-to-use (Dako).

Additionally, to evaluate the effect of different staining procedures, the staining for Ki-67 was carried out with a Dako Autostainer Link 48 (Dako) and a BenchMark Ultra (Ventana Medical Systems, Tucson, AZ) according to the manufacturer's instructions. The clone used in the autostainer was MIB-1 in Dako Autostainer Link 48, and it was 30-9 in BenchMark Ultra; the effect of the different clones was evaluated. Ki-67 stained slides were digitized using Hamamatsu NanoZoomer (Hamamatsu Photonics, Hamamatsu, Japan), and then Ki-67 positive nuclei were counted manually using the hot spot method.[19] High power ×40 field photos with 0.1 mm^2 field view were taken and all nuclei and Ki-67 positive nuclei were counted to evaluate Ki-67 positivity.

Nucleic acids extraction

Nucleic acids were extracted from 10 × 10 μm-thick sections for DNA and from 5 × 10 μm-thick sections for RNA using QIAamp DNA FFPE Tissue Kit (Qiagen, Tokyo, Japan) and RNeasy FFPE Kit (Qiagen), respectively.

PCR assays

DNA and RNA were assessed by PCR, and 1 μL of the sample was used as a PCR template. PCR was performed using the PrimeSTAR Max DNA Polymerase (Takara Bio, Shiga, Japan) according to the manufacturer's recommendations (thermal cycling conditions: 35 cycles of 98°C for 10 s, 55°C for 5 s, and 72°C for 5 s). RT-PCR was performed using the PrimeScript RT reagent Kit (Perfect Real Time) (Takara Bio, Shiga, Japan) for cDNA synthesis using random 6 mers according to the manufacturer's recommendations (thermal cycling conditions: 1 cycle of 37°C for 15 min and 85°C for 5 s). PCR amplification of ACTB (142 bp and 307 bp) and GAPDH (500 bp) were evaluated in genomic DNA. PCR amplification of GAPDH (142 bp) and TBP (161 bp, 252 bp, and 300 bp) were evaluated in cDNA. The 142 bp fragment of GAPDH and the 161 bp and 300 bp fragments of TBP span 1 intron, and the 252 bp fragment of TBP spans 2 intron sequences. The primer sequences are shown in Table S1.[20,21] Degraded DNA was evaluated using an Agilent 2100 Bioanalyzer (Agilent, Santa Clara, CA, USA).

Statistical analysis

To evaluate the effect of different type of formalin in the result of Ki-67 positivity, sections fixed with 10% NeuBF were used as a control, and the differences between the other types

were evaluated. To evaluate the effect of fixation time in the result of Ki-67 positivity, sections fixed for 24 h were used as a control, and sections fixed for 2 weeks were evaluated. To elucidate the effect of using an autostainer versus manual staining and of using different antibodies, manual staining was used as a control.

Student's *t*-test was used to determine statistically significance differences. The *P* value was set at 0.05.

RESULTS

Effect of pH and concentration of formalin in Ki-67 positivity

All sections under various fixation protocols showed nuclear expression in the basal crypt of epithelial cells in Ki-67 IHC. Figure 1 shows the Ki-67 positivity by fixation under different conditions such as various pHs, formalin concentrations, fixation times, and fixations by manual staining. Compared to the 10% NeuBF fixation, specimens fixed with the low pH formalin of pH 4 showed higher Ki-67 positivity in the 24 h and 48 h fixations. Ki-67 positivities in 10% NonBF for the 24 h and 48 h fixations, and in 10% formalin at pH 6 for the 48 h fixation, were significantly higher than that seen in 10% NeuBF ($P < 0.05$, Fig. 1a,b). The high pH formalin of pH 7 or pH 8 tended to show less Ki-67 positivity in the 1 week and 2 week fixations, but it was not statistically significant (Fig. 1c,d). Ki-67 positivity was not affected by 20% NeuBF and NonBF. Ki-67 positivity in all fixation protocols was low in the 2 week fixation when compared to the 1 week fixation. Furthermore, pH values of NonBF changed from 4 to 5 or 6 during the duration of the fixation (Fig. 1e,f).

Effect of fixation time in Ki-67 positivity

The effect of fixation time on Ki-67 positivity was evaluated under variable fixation times and using different staining procedures (Fig. 2). Ki-67 positivity was attenuated by longer fixation time, regardless of the difference in fixatives. Furthermore, this attenuation was notable after 1 or 2 week fixation (Fig. 2a). The same phenomenon was observed with either the manual or auto staining (Fig. 2b,c). And the same phenomenon was confirmed by using different antigen retrieval of pH 9 in manual staining. Sections treated with proteinase K for 3 min or 6 min were also performed, but positive stainings were not observed (Fig. 2d).

Effect of staining procedure

We evaluated the effect of the staining protocol between the manual and the autostaining system and also the effect of using different antibodies. Ki-67 positivity was compared between manual stained and Dako Autostainer Link 48 stained samples using the same MIB-1 antibody. Equivalent Ki-67 positivity was found between sections stained manually and with the Autostainer Link 48 (Fig. 3). In addition, regardless of the difference in the fixation protocol, similar Ki-67 positivity was observed between manual and Dako Autostainer Link 48 staining. The effect of different antibody clones on Ki-67 positivity was evaluated by using clones of MIB-1 (Dako) with manual staining and the Dako Autostainer Link 48, and by using 30-9 (Ventana) with the BenchMark Ultra. Ki-67 positivity was much higher in sections using 30-9 and stained by the BenchMark Ultra (Fig. 3). The same tendency was preserved with different fixation solutions. These results indicated that different clones also have an effect on Ki-67 positivity.

Figure 4 shows the immunohistochemical staining of the Ki-67 expressions with different fixatives and fixation periods. Ki-67 positivity and intensity of expression were different depending on the fixation protocols. The intensity of Ki-67 (MIB-1) expression in the section fixed by 10% NonBF was stronger than that seen in samples fixed by 10% NeuBF (Fig. 4a,b). Fixation for 24 h showed stronger intensity of Ki-67 (MIB-1) expression than that seen after 2 weeks of fixation (Fig. 4b,c). In addition, the intensity of clone 30-9 expression by BenchMark Ultra was stronger than that of MIB-1 and manual staining (Fig. 4a,d). These results show that not only positivity, but also the staining intensity, were influenced by the fixation protocol or staining procedure.

Effect of pH and concentration of formalin and fixation time on PCR assay

Genomic DNA and total RNA were extracted from blocks using the different fixation protocols. The results of PCR amplification of different fragment sizes are shown in Table 2. As for genomic DNA, the success rate of PCR assay was higher in 10% neutral or high pH formalin fixation than in low pH (pH 4.1) or 20% formalin fixation. In 10% NeuBF, 10% formalin at pH 7 or 8 fixations, PCR within 500 bp was successfully performed within 2 weeks of fixation time. In low pH and 20% formalin fixation, the success rate was lower depending on the fragment size and fixation time. As for the cDNA from mRNA, perfect amplification was observed only in short fragments within 252 bp. Fragments of 142 bp were successfully amplified within 48 h. The success rate was correlated with the small size of the fragment and short time of fixation. Figure 5 shows the degree of degradation of genomic DNA from NeuBF and NonBF under variable fixation times. Genomic DNA from NonBF increased low molecular weight smear depending on fixation times. Genomic DNA from 10% NeuBF was little affected by fixation times.

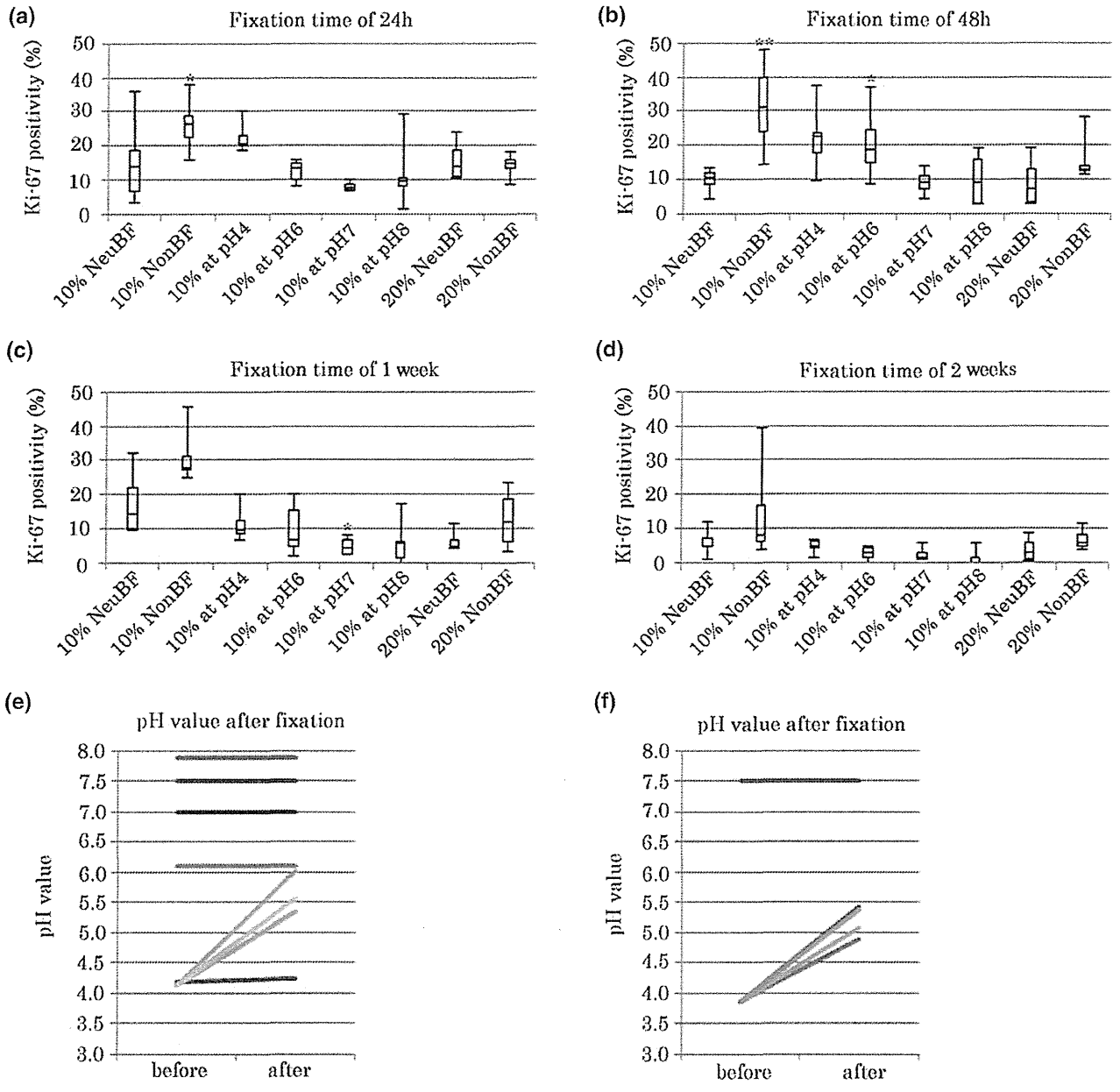

Figure 1 The effect of pH value and concentration in formalin with 24 h, 48 h, 1 week, and 2 week fixations by Ki-67 (MIB-1) manual staining. Box-and-whisker plots for comparison of the rate of Ki-67 positive nuclei stained manually in each fixative. Ki-67 (MIB-1) manually stained from specimens fixed (**a**) for 24 h, (**b**) for 48 h, (**c**) for 1 week, and (**d**) for 2 weeks. $^{*}P < 0.05$. $^{**}P < 0.01$. Change of pHvalue before and after fixation. (**e**) 10% NeuBF for 2 weeks; 10% with buffer at pH (4, 6, 7, and 8) for 2 weeks. 10% NonBF for 24 h, 48 h, 1 week and 2 weeks. (**f**) 20% NeuBF for 2 weeks; 20% NonBF for 24 h, 48 h, 1 week and 2 weeks. (**e**) —, 10% NeuBF 2w; —, 10% at pH4 2w; —, 10% at pH6 2w; —, 10% at pH7 2w; —, 10% at pH8 2w; —, 10% NonBF 24h; —, 10% NonBF 48h; —, 10% NonBF 1w; —, 10% NonBF 2w. (**f**) —, 20% NeuBF 2w; —, 20% NonBF 24h; —, 20% NonBF 48h; —, 20% NonBF 1w; —, 20% NonBF 2w.

DISCUSSION

Pathology laboratories are required to produce consistent data that are not affected by differences between laboratories. Recent progress in laboratory testing enables researchers to analyze not only protein expression but also DNA and mRNA assay from formalin fixed, paraffin-embedded tissue samples. Our study is the first to attempt to establish a standard fixation protocol suitable for multiple laboratory tests.

Ki-67 protein expression used in IHC has been utilized for multiple purposes including pathological diagnoses or therapeutic determinations in many types of cancers. Therefore,

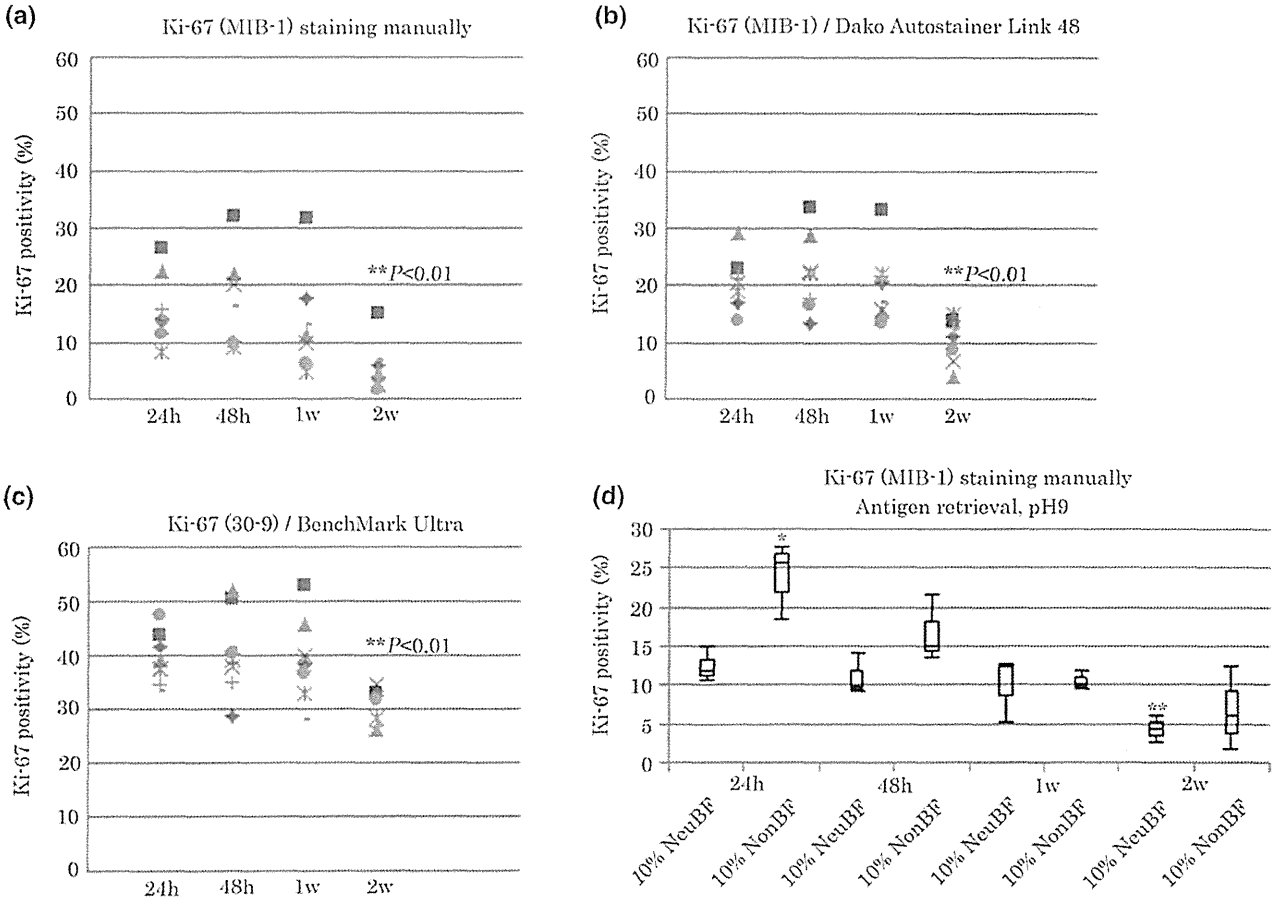

Figure 2 The effect of fixation time in Ki-67 (MIB-1) positivity using different staining procedures. Positive rate of (a) Ki-67 (MIB-1) staining manually, (b) Ki-67 (MIB-1) staining using Dako Autostainer Link 48, and (c) Ki-67 (30-9) staining using BenchMark Ultra with the change of fixaive time for each fixative. (d) The Ki-67 positivity by fixation under 10% NeuBF, 10%NonBF, various fixation times, and fixations by pH 9 antigen retrieval and manual staining. $*P < 0.05$. $**P < 0.01$. ◆, 10% NeuBF; ■, 10% NonBF; ▲, 10% at pH4; ✕, 10% at pH6; ✳, 10% at pH7; ●, 10% at pH8; +, 20% NeuBF; ═, 20% NonBF.

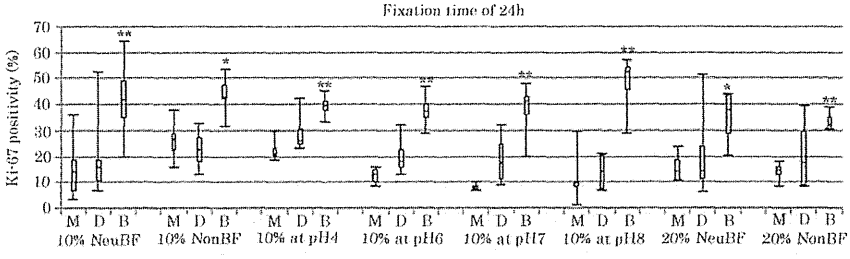

Figure 3 The effect of staining protocol using the autostaining system and different antibodies. Comparison of the positive rate of Ki-67 (MIB-1) staining manually (M), Ki-67 (MIB-1) staining using Dako Autostainer Link 48 (D) and Ki-67 (30-9) staining using BenchMark Ultra (B). $*P < 0.05$. $**P < 0.01$.

we selected the Ki-67 protein to study the effect of fixation protocols in protein assays. We evaluated the effect of acidity levels from pH 4 to pH 8, and Ki-67 positivity was strongly influenced by the pH level of the formalin. Furthermore, the pH value in non-buffered formalin changed during fixation. This result suggested that a neutral buffer is absolutely required to produce consistent data within different pathological laboratories, as reported in many recommendations.[2,11] The concentration of formalin can also be one of the important factors to be managed in pathology laboratories.[22] However, compared with pH or fixation time, the effect of fixation was not as substantial, at least between 10% and 20% formalin solutions. As for the fixation times, although Ki-67 is reported to be robust across fixation times, our results show marked reduction in the protein expression between 1 to 2 week fixation, regardless of the different

Table 2 PCR results in genomic DNA and cDNA

	Fixation	PCR results in genomic DNA			PCR results in cDNA			
Fixative	time	*ACTB* 142bp	*ACTB* 307bp	*GAPDH* 500bp	*GAPDH* 142bp	*TBP* 161bp	*TBP* 252bp	*TBP* 300bp
10% NeuBF								
	24h	100% ($n = 9$)	100% ($n = 9$)	100% ($n = 9$)	100% ($n = 9$)	100% ($n = 9$)	100% ($n = 9$)	0% ($n = 9$)
	48h	100% ($n = 3$)	100% ($n = 3$)	100% ($n = 3$)	100% ($n = 3$)	66.6% ($n = 3$)	66.6% ($n = 3$)	0% ($n = 3$)
	1w	100% ($n = 3$)	100% ($n = 3$)	100%($n = 3$)	100% ($n = 3$)	33.3% ($n = 3$)	0% ($n = 3$)	0% ($n = 3$)
	2w	100% ($n = 3$)	100% ($n = 3$)	100% ($n = 3$)	100% ($n = 3$)	66.6% ($n = 3$)	33.3% ($n = 3$)	0% ($n = 3$)
10% NonBF								
	24h	100% ($n = 3$)	100% ($n = 3$)	100%($n = 3$)	100% ($n = 3$)	66.6% ($n = 3$)	66.6% ($n = 3$)	0% ($n = 3$)
	48h	100% ($n = 3$)	100% ($n = 3$)	100% ($n = 3$)	100% ($n = 3$)	100% ($n = 3$)	66.6% ($n = 3$)	0% ($n = 3$)
	1w	50% ($n = 4$)	75% ($n = 4$)	0% ($n = 4$)	100% ($n = 4$)	0% ($n = 4$)	0% ($n = 4$)	0% ($n = 4$)
	2w	0% ($n = 3$)	0% ($n = 3$)	0% ($n = 3$)	100% ($n = 3$)	0% ($n = 3$)	0% ($n = 3$)	0% ($n = 3$)
10% at pH 4								
	24h	66.6% ($n = 3$)	66.6% ($n = 3$)	66.6% ($n = 3$)	100% ($n = 3$)	100% ($n = 3$)	66.6% ($n = 3$)	0% ($n = 3$)
	48h	66.6% ($n = 3$)	100% ($n = 3$)	33.3% ($n = 3$)	100% ($n = 3$)	100% ($n = 3$)	33.3% ($n = 3$)	0% ($n = 3$)
	1w	0% ($n = 3$)	0% ($n = 3$)	0% ($n = 3$)	100% ($n = 3$)	0% ($n = 3$)	0% ($n = 3$)	0% ($n = 3$)
	2w	0% ($n = 3$)	0% ($n = 3$)	0% ($n = 3$)	33.3% ($n = 3$)	0% ($n = 3$)	0% ($n = 3$)	0% ($n = 3$)
10% at pH 6								
	24h	100% ($n = 3$)	100% ($n = 3$)	100% ($n = 3$)	100% ($n = 3$)	100% ($n = 3$)	100% ($n = 3$)	66.6% ($n = 3$)
	48h	66.6% ($n = 3$)	100% ($n = 3$)	100% ($n = 3$)	100% ($n = 3$)	100% ($n = 3$)	100% ($n = 3$)	0% ($n = 3$)
	1w	100% ($n = 3$)	100% ($n = 3$)	100% ($n = 3$)	100% ($n = 3$)	66.6% ($n = 3$)	0% ($n = 3$)	0% ($n = 3$)
	2w	100% ($n = 3$)	100% ($n = 3$)	0% ($n = 3$)	100% ($n = 3$)	33.3% ($n = 3$)	0% ($n = 3$)	0% ($n = 3$)
10% at pH 7								
	24h	100% ($n = 3$)	100% ($n = 3$)	100% ($n = 3$)	100% ($n = 3$)	100% ($n = 3$)	100% ($n = 3$)	0% ($n = 3$)
	48h	100% ($n = 3$)	100% ($n = 3$)	100% ($n = 3$)	100% ($n = 3$)	100% ($n = 3$)	100% ($n = 3$)	0% ($n = 3$)
	1w	100% ($n = 3$)	100% ($n = 3$)	100% ($n = 3$)	100% ($n = 3$)	100% ($n = 3$)	33.3% ($n = 3$)	0% ($n = 3$)
	2w	100% ($n = 3$)	100% ($n = 3$)	100% ($n = 3$)	66.6% ($n = 3$)	33.3% ($n = 3$)	33.3% ($n = 3$)	0% ($n = 3$)
10% at pH 8								
	24h	100% ($n = 3$)	100% ($n = 3$)	100% ($n = 3$)	100% ($n = 3$)	100% ($n = 3$)	100% ($n = 3$)	0% ($n = 3$)
	48h	100% ($n = 3$)	100% ($n = 3$)	100% ($n = 3$)	100% ($n = 3$)	66.6% ($n = 3$)	33.3% ($n = 3$)	0% ($n = 3$)
	1w	100% ($n = 3$)	100% ($n = 3$)	100% ($n = 3$)	100% ($n = 3$)	33.3% ($n = 3$)	0% ($n = 3$)	0% ($n = 3$)
	2w	100% ($n = 3$)	100% ($n = 3$)	100% ($n = 3$)	100% ($n = 3$)	33.3% ($n = 3$)	0% ($n = 3$)	0% ($n = 3$)
20% NeuBF								
	24h	100% ($n = 3$)	100% ($n = 3$)	100% ($n = 3$)	100% ($n = 3$)	100% ($n = 3$)	100% ($n = 3$)	0% ($n = 3$)
	48h	100% ($n = 3$)	100% ($n = 3$)	100% ($n = 3$)	100% ($n = 3$)	100% ($n = 3$)	100% ($n = 3$)	0% ($n = 3$)
	1w	100% ($n = 3$)	100% ($n = 3$)	100% ($n = 3$)	100% ($n = 3$)	33.3% ($n = 3$)	0% ($n = 3$)	0% ($n = 3$)
	2w	100% ($n = 3$)	100% ($n = 3$)	33.3% ($n = 3$)	100% ($n = 3$)	33.3% ($n = 3$)	33.3% ($n = 3$)	0% ($n = 3$)
20% NonBF								
	24h	100% ($n = 3$)	100% ($n = 3$)	100% ($n = 3$)	100% ($n = 3$)	66.6% ($n = 3$)	33.3% ($n = 3$)	0% ($n = 3$)
	48h	66.6% ($n = 3$)	33.3% ($n = 3$)	33.3% ($n = 3$)	100% ($n = 3$)	100% ($n = 3$)	100% ($n = 3$)	0% ($n = 3$)
	1w	66.6% ($n = 3$)	0% ($n = 3$)	0% ($n = 3$)	66.6% ($n = 3$)	33.3% ($n = 3$)	0% ($n = 3$)	0% ($n = 3$)
	2w	0% ($n = 3$)	0% ($n = 3$)	0% ($n = 3$)	33.3% ($n = 3$)	0% ($n = 3$)	0% ($n = 3$)	0% ($n = 3$)

ACTB, beta-actin; GAPDH, glyceraldehyde 3-phosphate dehydrogenase; TBP, TATA-binding protein.

fixatives or clones used.[23] Therefore, fixation times no longer than 1 week can be a practical standard for IHC. Use of an autostainer can provide stable IHC data, and the consistent data between autostaining and manual staining supports the routine utility of an autostainer after the establishment of a proper staining protocol. However, the clones must be chosen carefully because Ki-67 positivity was different between clones of MIB-1 and 30-9. In addition, fixation with low pH showed higher Ki-67 positivity, but may not produce a consistent result. Therefore, we must be aware that a protocol with higher Ki-67 positivity may not always be the best to produce consistent data.

In addition to the IHC, DNA and RNA assays are increasingly required to be performed on one sample embedded in paraffin. In those cases, stable PCR gene amplification is required in the analytical phase. It has been reported that acidic pH levels cause degradation of nucleic acids, and we also confirmed that the success rate of PCR gene amplification was lower in a pH 4 fixation.[24] As for genomic DNA, using 10% and 20% NeuBF, we consistently performed PCR assays of DNA amplification for those fragments shorter than or equal to 500 bp that had been fixed for between 24 h to 1 week. These data also support the use of NeuBF. As for cDNA from mRNA, the amplification was largely dependent on the length of the product size. However, the shortest fragment of 142 bp was successfully amplified after 1 week in NeuBF. These results also indicated it would be practical to use NeuBF solution and fixation times of between 24 h to 1

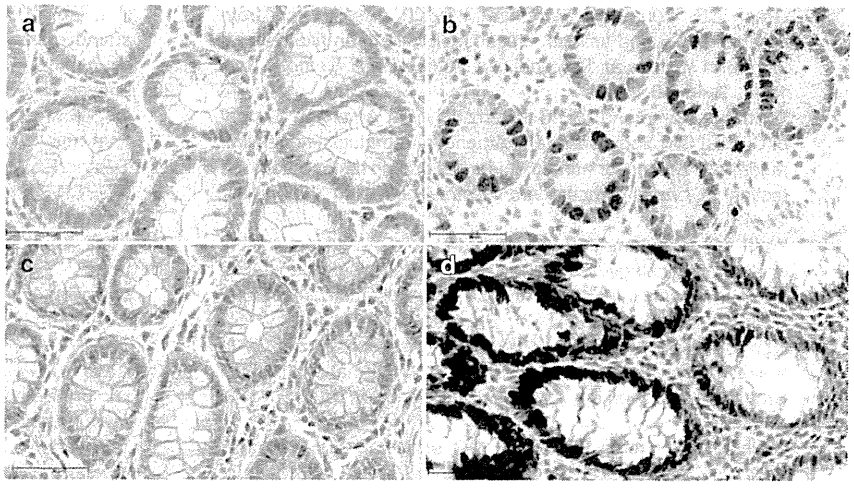

Figure 4 The immunohistochemical staining of Ki-67 expression with different fixatives and fixation periods. Ki-67 (MIB-1) staining manually (**a-c**), and Ki-67 (30-9) staining using BenchMark Ultra (**d**) of normal colonic mucosa according to the fixatives and fixation times. (**a, d**) 10% NeuBF for 24 h, (**b**) 10% NonBF for 24 h, (**c**) 10% with buffer at pH 4 for 2 weeks. Bar: 50 μm.

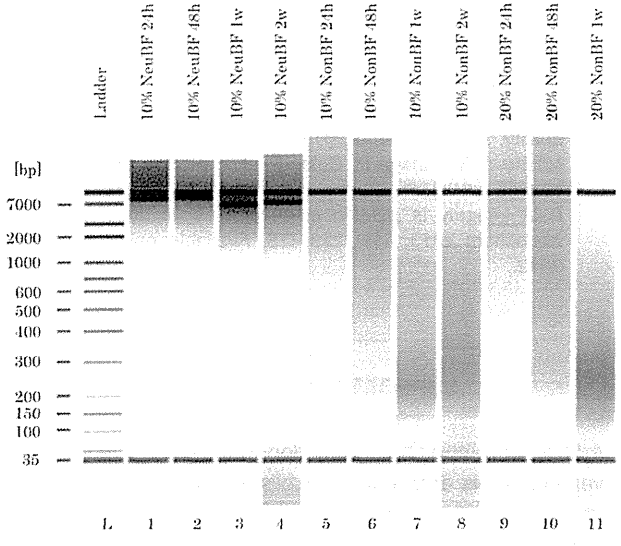

Figure 5 The degree of degradation of genomic DNA from NeuBF and NonBF under variable fixation times. L: Ladder; Lane 1: 10% NeuBF for 24 h; Lane 2: 10% NeuBF for 48 h; Lane 3: 10% NeuBF for 1 week; Lane 4: 10% NeuBF 2 weeks; Lane 5: 10% NonBF for 24 h; Lane 6: 10% NonBF for 48 h; Lane 7: 10% NonBF for 1 week; Lane 8: 10% NonBF for 2 weeks; Lane 9: 20% NonBF for 24 h; Lane 10: 20% NonBF for 48 h; Lane 11: 20% NonBF for 1 week.

week in the evaluation of DNA and RNA assays. Recently, alternative fixative with better preservation of nuclear acid than formaldehyde were reported.[25] Such a fixative may also be available when longer fragment analysis was required for the pathology laboratory in the future. On the other hand, at present, it is thought that NeuBF is a superior fixative for both protein and nucleic acids than NonBF.[26,27]

In conclusion, fixation protocols must be standardized to provide consistent result from multiple assays performed in different pathology laboratories. Taking these comprehensive results together, we recommend 10% NeuBF solution and fixation time of no longer than 1 week to obtain a uniform result in IHC, DNA, and RNA assays.

ACKNOWLEDGMENT

The authors thank Sachiko Fukuda for her excellent technical assistance. This study was supported in part by a Grant-in-Aid for Cancer Research (23-A-3) from the Ministry of Health, Labor and Welfare, Japan.

REFERENCES

1 Zarbo RJ. The oncologic pathology report. Quality by design. *Arch Pathol Lab Med* 2000; **124**: 1004–10.
2 Hammond ME, Hayes DF, Dowsett M *et al.* American Society of Clinical Oncology/College of American Pathologists guideline recommendations for immunohistochemical testing of estrogen and progesterone receptors in breast cancer (unabridged version). *Arch Pathol Lab Med* 2010; **134**: e48–72.
3 Matsuda Y, Fujii T, Suzuki T *et al.* Comparison of fixation methods for preservation of morphology, RNAs, and proteins from paraffin-embedded human cancer cell-implanted mouse models. *J Histochem Cytochem* 2011; **59**: 68–75.
4 Chung JY, Braunschweig T, Williams R *et al.* Factors in tissue handling and processing that impact RNA obtained from formalin-fixed, paraffin-embedded tissue. *J Histochem Cytochem* 2008; **56**: 1033–42.
5 Nykänen M, Kuopin T. Protein and gene expression of estrogen receptor alpha and nuclear morphology of two breast cancer cell lines after different fixation methods. *Exp Mol Pathol* 2010; **88**: 265–71.
6 DE Maezo AM, Fedor HH, Gage WR *et al.* Inadequate formalin fixation decreases reliability of p27 immunohistochemical staining: Probing optimal fixation time using high-density tissue microarrays. *Hum Pathol* 2002; **33**: 756–60.
7 Turashvili G, Yang W, McKinney S *et al.* Nucleic acid quantity and quality from paraffin blocks: Defining optimal fixation processing and DNA/RNA extraction techniques. *Exp Mol Pathol* 2012; **92**: 33–43.

8 Greer CE, Lund JK, Manos MM. PCR amplification from paraffin-embedded tissues: Recommendations on fixatives for long-term storage and prospective studies. *PCR Methods Appl* 1991; **1**: 46–50.
9 Wolff AC, Hammond ME, Schwartz JN *et al.* American Society of Clinical Oncology/College of American Pathologists guideline recommendations for human epidermal growth factor receptor 2 testing in breast cancer. *Arch Pathol Lab Med* 2007; **131**: 18–43.
10 Wolff AC, Hammond ME, Schwartz JN *et al.* American Society of Clinical Oncology/College of American Pathologists guideline recommendations for human epidermal growth factor receptor 2 testing in breast cancer. *J Clin Oncol* 2007; **25**: 118–45.
11 Dowsett M, Nielsen TO, A'Hern R *et al.* Assessment of Ki67 in breast cancer: Recommendations from the International Ki67 in Breast Cancer working group. *J Natl Cancer Inst* 2011; **103**: 1656–64.
12 Nakhleh RE, Grimm EE, Idowu MO *et al.* Laboratory compliance with the American Society of Clinical Oncology/college of American Pathologists guidelines for human epidermal growth factor receptor 2 testing: A College of American Pathologists survey of 757 laboratories. *Arch Pathol Lab Med* 2010; **134**: 728–34.
13 Hewitt SM, Lewis FA, Cao Y *et al.* Tissue handling and specimen preparation in surgical pathology: Issue concerning the recovery of nucleic acids from formalin-fixed, paraffin-embedded tissue. *Arch Pathol Lab Med* 2008; **132**: 1929–35.
14 Renne R, Fouillet X, Maurer J *et al.* Recommendation of optimal method for formalin of rodent lungs in routine toxicology studies. *Toxicol Pathol* 2001; **29**: 587–9.
15 Nofech-Mozes S, Vella ET, Dhesy-Thind S *et al.* Cancer care ontario guideline recommendations for hormone receptor testing in breast cancer. *Clin Oncol* 2012; **24**: 684–96.
16 Summary of ASCO/CAP HER2 Guideline Recommendations. (Accessed 6 September 2011.) Available from: http://www.cap.org/apps/docs/committees/immunohistochemistry/summary_of_recommendations.pdf
17 CAP Home. KRAS Mutation Testing for Colorectal Cancer (CRC). (Accessed 17 December 2010.) Available from: http://www.cap.org/apps/cap.portal
18 CAP Home. Frequently Asked Questions About ER/PgR Testing Guidelines. (Accessed 12 January 2011.) Available from: http://www.cap.org/apps/cap.portal
19 Preusser M, Heinzl H, Gelpi E *et al.* Ki67 index in intracranial ependymoma: A promising histopathological candidate biomarker. *Histopathology* 2008; **53**: 39–47.
20 Ludyga N, Grünwald B, Azimzadeh O *et al.* Nucleic acids from long-term preserved FFPE tissues are suitable for downstream analyses. *Virchows Arch* 2012; **460**: 131–40.
21 Takano EA, Mikeska T, Dobrovic A *et al.* A multiplex endpoint RT-PCR assay for quality assessment of RNA extracted from formalin-fixed paraffin-embedded tissues. *BMC Biotechnol* 2010; **10**: 89.
22 Engel KB, Moore HM. Effects of preanalytical variables on the detection of proteins by immunohistochemistry in formalin-fixed, paraffin-embedded tissue. *Arch Pathol Lab Med* 2011; **135**: 537–43.
23 Arber DA. Effect of prolonged formalin fixation on the immunohistochemical reactivity of breast markers. *Appl Immunohistochem Mol Morphol* 2002; **10**: 183–6.
24 Srinivasan M, Sedmak D, Jewell S. Effect of fixatives and tissue processing on the content and integrity of nucleic acids. *Am J Pathol* 2002; **161**: 1961–71.
25 Staff S, Kujala P, Karhu R *et al.* Preservation of nucleic acids and tissue morphology in paraffin-embedded clinical samples: Comparison of five molecular fixatives. *J Clin Pathol* 2013; **66**: 807–10.
26 Groelz D, Sobin L, Branton P *et al.* Non-formalin fixative versus formalin-fixed tissue: A comparison of histology and RNA quality. *Exp Mol Pathol* 2013; **94**: 188–94.
27 Milcheva R, Janega P, Celec P *et al.* Alcohol based fixatives provide excellent morphology, protein immunoreactivity and RNA integrity in paraffin embedded tissue specimens. *Acta Histochem* 2013; **115**: 279–115. Available online 24 August 2012.

SUPPORTING INFORMATION

Additional Supporting Information may be found in the online version of this article at the publisher's web-site:

Table S1 The primer sequences information.

European Journal of Cancer (2014) 50, 1900–1908

Available at www.sciencedirect.com

ScienceDirect

journal homepage: www.ejcancer.com

Prognostic impact of M2 macrophages at neural invasion in patients with invasive ductal carcinoma of the pancreas

Motokazu Sugimoto [a,b,d], Shuichi Mitsunaga [a,c], Kiyoshi Yoshikawa [a], Yuichiro Kato [b], Naoto Gotohda [b], Shinichiro Takahashi [b], Masaru Konishi [b], Masafumi Ikeda [c], Motohiro Kojima [a], Atsushi Ochiai [a,*], Hironori Kaneko [d]

[a] *Division of Pathology, Research Center for Innovative Oncology, National Cancer Center Hospital East, Japan*
[b] *Department of Hepatobiliary and Pancreatic Surgery, National Cancer Center Hospital East, Japan*
[c] *Department of Hepatobiliary and Pancreatic Oncology, National Cancer Center Hospital East, Japan*
[d] *Department of Surgery, Toho University School of Medicine, Japan*

Received 11 March 2014; accepted 9 April 2014
Available online 15 May 2014

KEYWORDS
Pancreatic cancer
Pancreaticoduodenectomy
Neural invasion
M2 macrophages
Overall survival
Peritoneal dissemination
Locoregional recurrence
Adjuvant chemotherapy

Abstract ***Background:*** Neural invasion is a characteristic pattern of invasion and an important prognostic factor for invasive ductal carcinoma (IDC) of the pancreas. M2 macrophages have reportedly been associated with poor prognosis in various cancers. The aim of the present study was to investigate the prognostic impact of M2 macrophages at extrapancreatic nerve plexus invasion (plx-inv) of pancreatic IDC.

Methods: Participants comprised 170 patients who underwent curative pancreaticoduodenectomy for pancreatic IDC. Immunohistochemical examination of surgical specimens was performed by using CD204 as an M2 macrophage marker, and the area of immunopositive cells was calculated automatically. Prognostic analyses of clinicopathological factors including CD204-positive cells at plx-inv were performed.

Results: Plx-inv was observed in 91 patients (53.5%). Forty-eight patients showed a high percentage of CD204-positive cell area at plx-inv (plx-inv CD204%^{high}). Plx-inv CD204%^{high} was an independent predictor of poor outcomes for overall survival (OS) ($P < 0.001$) and disease-free survival (DFS) ($P < 0.001$). Patients with plx-inv CD204%^{high} showed a shorter time to peritoneal dissemination ($P < 0.001$) and locoregonal recurrence ($P < 0.001$). In patients who underwent adjuvant chemotherapy, plx-inv CD204%^{high} was correlated with shorter OS ($P = 0.011$) and DFS ($P = 0.038$) in multivariate analysis.

* *Corresponding author:* Address: National Cancer Center Hospital East, 6-5-1 Kashiwa-no-ha, Kashiwa, Chiba 277-8577, Japan. Tel.: +81 4 7134 6855; fax: +81 4 7134 6865.
E-mail address: aochiai@east.ncc.go.jp (A. Ochiai).

http://dx.doi.org/10.1016/j.ejca.2014.04.010

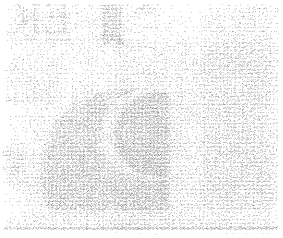

Conclusions: Plx-inv CD204%^{high} was associated with shortened OS and DFS and early recurrence in the peritoneal cavity and locoregional space. The prognostic value of plx-inv CD204%^{high} was also applicable to patients who received adjuvant chemotherapy. High accumulation of M2 macrophages at plx-inv represents an important predictor of poor prognosis.

1. Introduction

Pancreatic cancer is an aggressive malignancy with a high incidence of recurrence and low rates of survival, even when curative resection is achieved [1,2]. However, the mechanisms underlying this intractability have yet to be elucidated. Neural invasion has been accepted as an important prognostic factor for invasive ductal carcinoma (IDC) of the pancreas [3–7]. Patients with severe neural invasion are categorised as unresectable cases [8] and experience pain, cachexia, peritoneal dissemination and poor prognosis [9–11].

In vivo and *in vitro* models have been established to shed light on the mechanisms underlying neural invasion [9,12–15]. In our previous study [12], highly expressed genes in nerve tissues of the mouse model using Capan-1, a human pancreatic cancer cell line, included macrophage-related genes such as lysozyme [16], macrophage-expressed gene 1 glycoprotein [16] and early growth response 1 [17]. In other experimental studies, the paracrine regulation of neurotrophins was associated with the recruitment of macrophages in neural invasion and the migration of tumour cells [14,15]. Accumulation of macrophages at sites of neural invasion is considered to support tumour cell proliferation and is presumably related to poor prognosis.

Macrophages that have infiltrated into cancer stroma are termed tumour-associated macrophages (TAMs) and promote tumour progression and metastasis [18]. Increased density of TAMs is associated with poor prognosis in cancers of the thyroid, prostate, stomach, bile duct and pancreas [19–23]. TAMs express an M2-skewed phenotype, which is activated in chronic inflammation, scavenge debris and promote angiogenesis and tissue remodelling [18]. M2 macrophages show high expression of scavenger receptor (SR)-A (CD204). High accumulation of CD204-positive cells at the periphery of pancreatic IDC was correlated with shorter overall survival (OS) and disease-free survival (DFS) in our previous study [23]. However, to the best of our knowledge, the clinical impact of M2 macrophages in neural invasion sites has not been elucidated in any kind of malignancies. The aim of the present study was to investigate the prognostic value of M2 macrophages at neural invasion in patients with pancreatic IDC who underwent curative pancreaticoduodenectomy.

2. Methods

2.1. Patients

A total of 177 patients underwent curative (R0) pancreaticoduodenectomy and were histologically diagnosed with pancreatic IDC at our institution between September 1992 and June 2011. Seven patients were excluded due to surgical mortality ($n = 3$), incomplete follow-up data ($n = 2$) and poor-quality surgical specimens ($n = 2$). The remaining 170 patients were included in this investigation. The median patient age at the time of surgery was 65 years [range, 34–84 years], and 63 (37.1%) were women. Sixty patients received postoperative adjuvant chemotherapy, consisting of gemcitabine in 40 patients (66.7%), S-1 (an oral fluoropyrimidine) in 10 (16.7%), gemcitabine plus S-1 in 6 (10.0%) and 5-fluorouracil plus cisplatin in 4 (6.7%). Inclusion criteria for adjuvant chemotherapy basically conformed to the criteria of the nationwide Japanese randomised phase III trial [24]. Neoadjuvant therapy was performed in four patients. Lymphadenectomy was performed according to the Japanese General Rules for the Study of Pancreatic Cancer [25]. All patients signed an institutional review board-approved informed consent form.

2.2. Evaluation of clinicopathological features

Each resected specimen was fixed in 10% formalin at room temperature, and the size and gross appearance of the tumour were recorded [3]. The entire tumour was cut at intervals of 0.5–0.7 cm, and the specimens were routinely processed and embedded in paraffin. Serial sections (3-μm thick) of each tumour were cut, and one section was stained with haematoxylin and eosin (HE). Histopathological findings were examined according to the definitions of the Japan Pancreas Society [25]. The following clinicopathological factors were investigated to assess their prognostic value: age; sex; Eastern Cooperative Oncology Group performance status (ECOG PS); presence of adjuvant chemotherapy; serum level of carcinoembryonic antigen (CEA); serum level of carbohydrate antigen (CA)19-9; tumour differentiation; tumour size; serosal invasion; retroperitoneal invasion; portal vein invasion; lymphatic invasion (ly); vessel invasion (v); intrapancreatic neural invasion (ne); lymph node involvement and extrapancreatic nerve plexus invasion

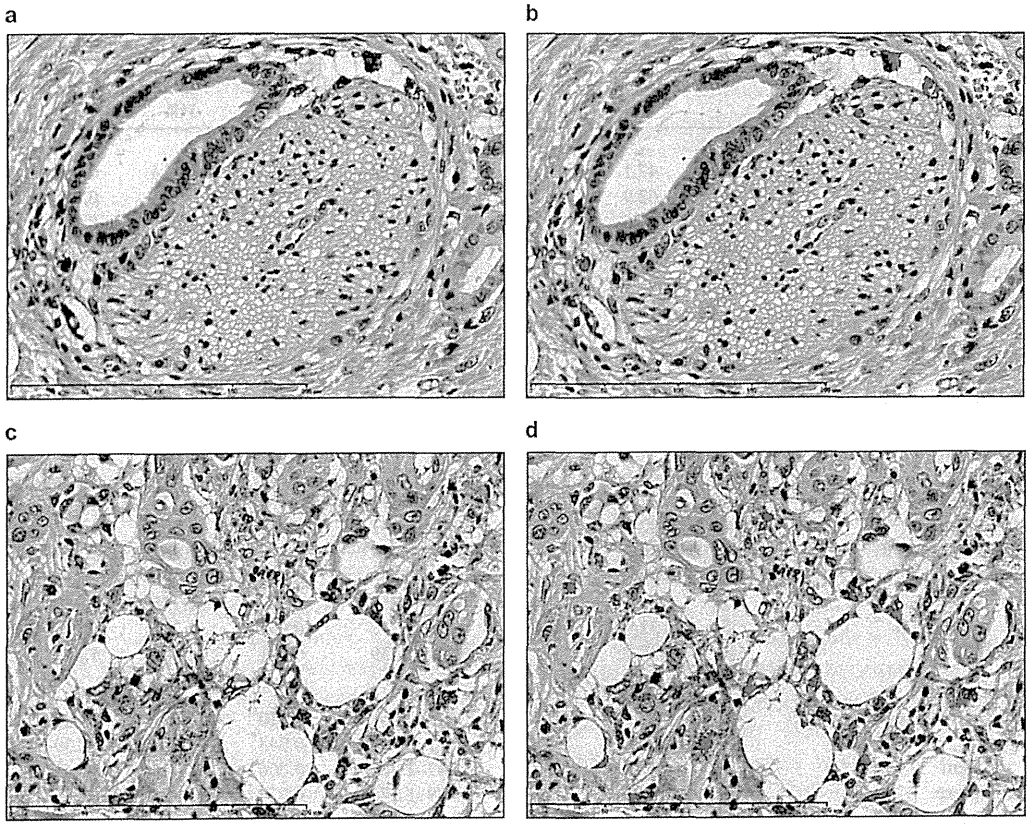

Fig. 1. (a) CD204-positive cells at an extrapancreatic nerve plexus invasion (plx-inv) (magnification, ×400). (b) Red areas represent CD204-positive cells, and the percentage area of CD204-positive cells was calculated as (area of CD204-positive cells/measured area) × 100 using the automeasure function in Axio Vision 4.7.1 software (Carl Zeiss, Oberkochen, Germany). (c) CD204-positive cells at the tumour periphery (magnification, ×400). (d) CD204-positive cells are expressed as red areas.

(plx-inv). Ly, v and ne were classified into four groups based on the most extensively involved area observed under low-power magnification (×100): no invasion of cancer cells; slight invasion of a few cancer cells (1–3 points); moderate invasion (4–8 points) and severe invasion (>8 points). Pathological stage was evaluated according to the 7th edition of the International Union Against Cancer (UICC) classification (IA/IB/IIA versus IIB/III/IV) [26]. Cut-off values for continuous variables were determined from median values for all patients.

2.3. Definition of the tumour periphery and plx-inv

HE-stained sections at the maximal diameter of the tumour were evaluated at a magnification of ×40, and the margin of the tumour was marked on each slide. The periphery of the primary tumour was defined as fields that included cancer cells and adjacent non-cancerous cells at a magnification of ×100 [23]. As described in our previous study [3], plx-inv was defined as invasion of tumour cells inside the perineurium, apart from both the pancreatic capsule and main tumour, and was evaluated at a magnification of ×400 in all sections. Plx-inv distance was defined as the distance from the plx-inv to the main tumour. The cut-off for plx-inv distance was set at 2500 μm, and the prognostic value was evaluated [3].

2.4. Immunohistochemical staining and evaluation

Mouse anti-human CD204 antibody (Scavenger Receptor class A-E5, 1:400 in blocking buffer; Transgenic, Kumamoto, Japan) was used for immunohistochemical staining [23]. The percentage area of CD204-positive cells (CD204%) was calculated as (area of CD204-positive cells/measured area) × 100 using the automeasure function in Axio Vision 4.7.1 software (Carl Zeiss, Oberkochen, Germany) [23]. The mean CD204% for three hot spots at the tumour periphery and plx-inv was calculated in each patient. Median CD204% for all patients with plx-inv was used to determine CD204%^{high} as equal to or above the median. Prognostic analyses for CD204%^{high} at the periphery and plx-inv were performed.

2.5. Assessment of recurrence

Contrast-enhanced computed tomography or magnetic resonance imaging was performed every 3 months after surgery. Sites of recurrence were categorised as

Table 1
Prognostic analyses for overall survival and disease-free survival in patients with invasive ductal carcinoma of the pancreas ($n = 170$).

Parameter	*n*	%	Overall survival			Disease-free survival		
			HR	95% CI	P	HR	95% CI	P
(a) Univariate analysis								
Age ⩾ 65	80	47.1	1.077	0.775–1.498	0.657	1.114	0.808–1.535	0.510
Sex, male	107	62.9	0.876	0.625–1.227	0.442	0.960	0.689–1.339	0.811
ECOG PS ⩾ 1	28	16.5	1.975	1.266–3.081	0.003*	1.403	0.909–2.166	0.126
Absence of adjuvant chemotherapy	110	64.7	1.715	1.186–2.481	0.004*	1.501	1.061–2.123	0.022*
CEA ⩾ 3.4 ng/ml	88	51.8	1.419	1.019–1.975	0.038*	1.584	1.147–2.186	0.005*
CA19-9 ⩾ 111.5 U/ml	85	50.0	0.904	0.648–1.260	0.550	1.026	0.743–1.417	0.877
Tumour differentiation, moderate/poor	126	74.1	1.248	0.857–1.817	0.248	1.514	1.042–2.199	0.030*
Tumour size ⩾ 3.0 cm	81	47.6	1.615	1.160–2.248	0.005*	1.596	1.156–2.203	0.004*
Serosal invasion (+)	46	27.1	0.865	0.591–1.266	0.457	1.164	0.811–1.671	0.411
Retroperitoneal invasion (+)	145	85.3	1.174	0.724–1.904	0.516	1.060	0.668–1.682	0.805
Portal vein invasion (+)	40	23.5	1.479	1.014–2.156	0.042*	1.186	0.818–1.722	0.368
Ly, moderate to severe	46	27.1	1.634	1.130–2.365	0.009*	1.620	1.135–2.312	0.008*
V, moderate to severe	103	60.6	1.779	1.254–2.524	0.001*	1.636	1.168–2.292	0.004*
Ne, moderate to severe	106	62.4	1.812	1.270–2.583	0.001*	1.637	1.164–2.302	0.005*
Lymph node involvement (+)	141	82.9	1.505	0.968–2.341	0.069	1.554	1.002–2.409	0.049*
Pathological stage IIB/III/IV	143	84.1	1.414	0.903–2.214	0.130	1.463	0.937–2.284	0.094
Peripheral CD204%^{high}	85	50.0	1.777	1.272–2.484	0.001*	1.570	1.135–2.172	0.006*
Plx-inv (+)	91	53.5	1.612	1.147–2.264	0.006*	1.785	1.280–2.489	0.001*
Plx-inv distance ⩾ 2500 μm	56	32.9	1.949	1.368–2.777	<0.001*	2.274	1.597–3.238	<0.001*
Plx-inv CD204%^{high}	48	28.2	1.779	1.247–2.539	0.001*	1.904	1.341–2.705	<0.001*
(b) Multivariate analysis								
Absence of adjuvant chemotherapy	110	64.7	1.741	1.143–2.651	0.010*	1.559	1.042–2.332	0.031*
CEA ⩾ 3.4 ng/ml	88	51.8	1.437	1.011–2.041	0.043*	1.602	1.139–2.253	0.007*
Tumour size ⩾ 3.0 cm	81	47.6	1.610	1.147–2.262	0.006*	1.616	1.160–2.250	0.005*
Ly, moderate to severe	46	27.1	1.254	0.839–1.876	0.270	1.151	0.775–1.709	0.487
V, moderate to severe	103	60.6	1.505	1.010–2.242	0.045*	1.291	0.879–1.897	0.192
Peripheral CD204%^{high}	85	50.0	2.167	1.522–3.086	<0.001*	1.831	1.297–2.583	0.001*
Plx-inv CD204%^{high}	48	28.2	2.008	1.362–2.962	<0.001*	2.046	1.400–2.991	<0.001*

* $P < 0.05$. Prognostic analyses were carried out using Cox regression model. HR, hazard ratio; 95% CI, 95% confidence interval; ECOG PS, Eastern Cooperative Oncology Group performance status; CEA, carcinoembryonic antigen; CA19-9, carbohydrate antigen 19-9; Ly, lymphatic invasion; V, vessel invasion; Ne, intrapancreatic neural invasion, Peripheral CD204%^{high}, percentage of CD204-positive cells area at the periphery ⩾ 3.34; Plx-inv, extrapancreatic nerve plexus invasion; Plx-inv CD204%^{high}, percentage of CD204-positive cells area at plx-inv ⩾ 0.57.

liver metastasis, peritoneal dissemination, locoregional recurrence and distant lymph node metastasis. Peritoneal dissemination was defined as marked peritoneal nodules, increased ascites or malignant ascites as confirmed by cytology. Locoregional recurrence was defined as tumour in a dissected space or metastasis in regional lymph nodes according to the 7th edition of the UICC classification [26]. Distant lymph node metastasis was defined as marked lymph node swelling apart from the regional space.

2.6. Statistical analysis

Uni- and multivariate analyses for OS, DFS and time to each type of recurrence were performed using a Cox regression model. Factors showing values of $P < 0.05$ for both OS and DFS in univariate analyses were included in multivariate analyses. Pearson's correlation coefficient r was used to evaluate the correlation among covariates. The observation period was until March 2013, and the median duration was 17.6 months [95% confidence interval (CI), 14.5–20.6]. OS was defined as the time from surgery to death or the date censored at last follow-up. DFS was calculated as the time from surgery to tumour relapse or death or the date censored at last follow-up. Survival curves were drawn using the Kaplan–Meier method, and the differences between patient groups were analysed by log-rank test. *P*-values were two-sided, with the significance level at $P < 0.05$. Statistical analyses were performed using SPSS version 19.0 software (SPSS, Chicago, IL).

3. Results

3.1. Distribution of CD204%

CD204 accumulation at the primary tumour was measured in all 170 patients, and median CD204% at the tumour periphery was 3.34% [range, 0.16–14.04%]. Plx-inv was observed in 91 patients (53.5%). CD204-positive cells and the measured area at plx-inv are shown in Fig. 1a and b, and CD204-positive cells and the measured area at the tumour periphery are shown in Fig. 1c and d. Median CD204% at plx-inv was 0.57% [range,

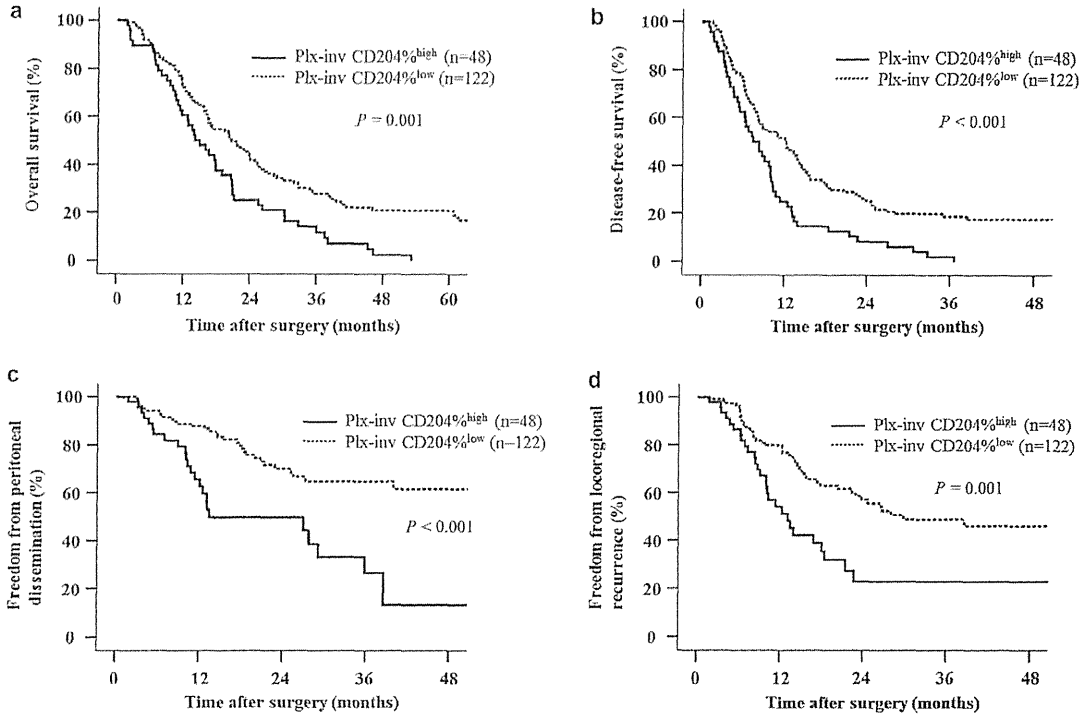

Fig. 2. (a) Kaplan–Meier curve for overall survival stratified by the level of CD204-positive cell area as a percentage at extrapancreatic nerve plexus invasion (plx-inv CD204%). (b) Kaplan–Meier curve for disease-free survival stratified by the level of CD204-positive cell area as a percentage at extrapancreatic nerve plexus invasion (plx-inv CD204%). (c) Kaplan–Meier curve for peritoneal dissemination-free survival stratified by the level of CD204-positive cell area as a percentage at extrapancreatic nerve plexus invasion (plx-inv CD204%). (d) Kaplan–Meier curve for locoregional recurrence-free survival stratified by the level of CD204-positive cell area as a percentage at extrapancreatic nerve plexus invasion (plx-inv CD204%).

0.00–7.76%]. Forty-eight patients with CD204% at plx-inv $\geqslant$0.57% were categorised as plx-inv CD204%^{high}. There were 43 patients with CD204% at plx-inv <0.57% and 79 patients without plx-inv, who were categorised as plx-inv CD204%^{low}.

3.2. Prognostic analyses of clinicopathological factors

The median OS and DFS were 17.8 months [95% CI, 14.7–20.9] and 9.8 months [95% CI, 7.9–11.6], respectively. Univariate analysis identified absence of adjuvant chemotherapy, CEA $\geqslant$ 3.4 ng/ml, tumour size $\geqslant$ 3.0 cm, moderate to severe ly, v and ne, peripheral CD204%^{high}, plx-inv, plx-inv distance $\geqslant$ 2500 μm and plx-inv CD204%^{high} as candidates for correlation with both shorter OS and shorter DFS ($P < 0.05$) (Table 1a). Strong correlations were observed between plx-inv CD204%^{high} and the following covariates: moderate to severe ne, $r = 0.299$, $P < 0.001$; plx-inv, $r = 0.584$, $P < 0.001$; and plx-inv distance $\geqslant$ 2500 μm, $r = 0.534$, $P < 0.001$. Therefore, these covariates were excluded from the multivariate analysis. Multivariate analysis revealed absence of adjuvant chemotherapy (hazard ratio [HR], 1.741; $P = 0.010$), CEA $\geqslant$ 3.4 ng/ml (HR, 1.437; $P = 0.043$), tumour size $\geqslant$ 3.0 cm (HR, 1.610; $P = 0.006$), moderate to severe v (HR, 1.505; $P = 0.045$), peripheral CD204%^{high} (HR, 2.167; $P < 0.001$), and plx-inv CD204%^{high} (HR, 2.008; $P < 0.001$) as independent risk factors for shorter OS (Table 1b). In terms of DFS, absence of adjuvant chemotherapy (HR, 1.559; $P = 0.031$), CEA $\geqslant$ 3.4 ng/ml (HR, 1.602; $P = 0.007$), tumour size $\geqslant$ 3.0 cm (HR, 1.616; $P = 0.005$), peripheral CD204%^{high} (HR, 1.831; $P = 0.001$) and plx-inv CD204%^{high} (HR, 2.046; $P < 0.001$) represented independent risk factors for shorter DFS (Table 1b). OS and DFS curves according to the level of plx-inv CD204% are shown in Fig. 2a and b.

3.3. Time to relapse according to site of recurrence

Median times to tumour relapse were 7.3 months [95% CI, 5.5–9.1] for liver metastasis (71 patients, 41.8%), 12.1 months [9.2–15.0] for peritoneal dissemination (57 patients, 33.5%), 10.0 months [7.1–13.0] for locoregional recurrence (76 patients, 44.7%) and 8.8 months [4.0–13.6] for distant lymph node recurrence (46 patients, 27.1%). Multivariate analyses showed that absence of adjuvant chemotherapy (HR, 1.924; $P = 0.030$) and moderate to severe ly (HR, 2.634; $P < 0.001$) correlated with early relapse to liver metastasis (Table 2). Peripheral CD204%^{high} was a predictor of peritoneal dissemination (HR, 1.815; $P = 0.031$)

(Table 2). Plx-inv CD204%^{high} was independently associated with peritoneal dissemination (HR, 2.886; $P < 0.001$) and locoregional recurrence (HR, 2.483; $P < 0.001$) (Table 2 and Fig. 2c and d).

3.4. Prognostic analyses stratified by presence of adjuvant chemotherapy

Adjuvant chemotherapy represented an independent prognostic factor for OS and DFS as a definitive therapeutic modality (Table 1, Fig. 3a and b). Multivariate analyses to test prognostic factors with adjuvant chemotherapy were re-examined and revealed that only plx-inv CD204%^{high} was associated with both shorter OS (HR, 2.624; $P = 0.011$) and shorter DFS (HR, 2.257; $P = 0.038$) in patients with plx-inv who underwent postoperative adjuvant chemotherapy (Table 3).

4. Discussion

The present study demonstrated that the accumulation of CD204-positive cells, representing M2 macrophages, at plx-inv of pancreatic IDC was an independent predictor of shorter OS and DFS in patients who underwent curative pancreaticoduodenectomy for pancreatic IDC. The prognostic impact of plx-inv CD204%^{high} was maintained in patients who received adjuvant chemotherapy. Infiltration of M2 macrophages at plx-inv of pancreatic IDC was revealed as a key factor to explain the aggressiveness of pancreatic IDC for the first time in this study.

Peritoneal dissemination has long been considered a poor prognostic factor for patients with pancreatic IDC [27–29]. Patients with plx-inv CD204%^{high} showed early relapse to the peritoneal cavity in this study. The interaction between M2 macrophages and tumour cells at plx-inv was suggested to play a crucial role in peritoneal recurrence, which led to poor survival. From the perspective of surgical anatomy, nerve fibres of the plexus pancreaticus capitalis might provide a convenient pathway for infiltrating tumour cells. As recent experimental study showed that macrophages around nerves were recruited in response to cytokine secreted by invading tumour cells and increased migration of tumour cells [15], M2 macrophages might promote the invasiveness of tumour cells at plx-inv, leading tumour cells to disperse into the peritoneal space and resulting in peritoneal dissemination. This speculation warrants further studies to observe the distribution of M2 macrophages in metastatic sites of pancreatic IDC and to test the role of M2 macrophages in metastatic tumour models.

Immunophysiologically, neural injury leads to the accumulation of macrophages in the peripheral nerve system, although few macrophages exist in intact nerves [30]. Ceyhan et al. reported that neuritis was caused by the invasion of malignant tumour cells into the pancreas

Table 2
Multivariate analysis for early relapse according to the sites of recurrence in patients with invasive ductal carcinoma of the pancreas ($n = 170$).

Parameter	Liver metastasis ($n = 71$)				Peritoneal dissemination ($n = 57$)				Locoregional recurrence ($n = 76$)				Distant lymph node metastasis (n = 46)			
	n	%	HR	95% CI	P	n	%	HR	95% CI	P	n	%	HR	95% CI	P	n	%	HR	95% CI	P
Absence of adjuvant chemotherapy	50	70.4	1.924	1.065–3.476	0.030*	34	59.6	1.107	0.602–2.036	0.743	52	68.4	1.734	0.995–3.022	0.052	32	69.6	1.660	0.794–3.471	0.178
CEA ⩾ 3.4 ng/ml	40	56.3	1.347	0.819–2.215	0.241	23	40.4	0.934	0.531–1.640	0.811	36	47.4	1.238	0.773–1.985	0.374	26	56.5	1.516	0.810–2.839	0.193
Tumour size ⩾ 3.0 cm	38	53.5	1.492	0.925–2.405	0.101	22	38.6	0.968	0.558–1.681	0.909	34	44.7	1.114	0.698–1.780	0.650	23	50.0	1.327	0.732–2.407	0.351
Ly, moderate to severe	28	39.4	2.634	1.574–4.408	<0.001*	14	24.6	0.839	0.436–1.617	0.601	21	27.6	0.878	0.501–1.539	0.649	17	37.0	1.909	0.993–3.671	0.053
V, moderate to severe	46	64.8	1.146	0.660–1.988	0.629	30	52.6	1.126	0.618–2.052	0.698	47	61.8	1.323	0.774–2.261	0.306	29	63.0	1.133	0.560–2.292	0.729
Peripheral CD204%^{high}	37	52.1	1.517	0.931–2.472	0.095	30	52.6	1.815	1.055–3.124	0.031*	36	47.4	1.501	0.933–2.417	0.094	21	45.7	1.305	0.706–2.412	0.396
Plx-inv CD204%^{high}	18	25.4	0.916	0.518–1.619	0.763	24	42.1	2.886	1.615–5.159	<0.001*	28	36.8	2.483	1.485–4.151	<0.001*	15	32.6	1.564	0.795–3.073	0.195

* $P < 0.05$. Multivariate analysis was carried out using Cox regression hazard model. HR, hazard ratio; 95% CI, 95% confidence interval; CEA, carcinoembryonic antigen; Ly, lymphatic invasion; V, vessel invasion; Peripheral CD204%^{high}, percentage of CD204-positive cells area at the periphery ⩾ 3.34; Plx-inv CD204%^{high}, percentage of CD204-positive cells area at extrapancreatic nerve plexus invasion ⩾ 0.57.

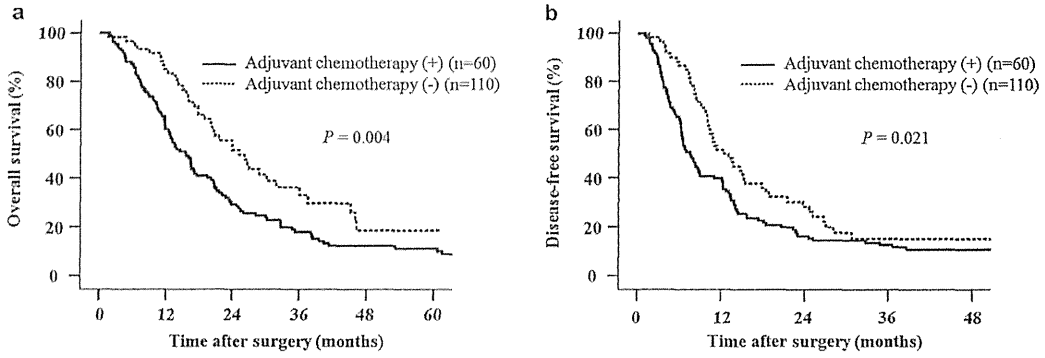

Fig. 3. (a) Kaplan–Meier curve for overall survival stratified by the presence of adjuvant chemotherapy. (b) Kaplan–Meier curve for disease-free survival stratified by the presence of adjuvant chemotherapy.

Table 3
Multivariate analysis for overall survival and disease-free survival in patients who received adjuvant chemotherapy ($n = 60$).

Parameter	n	%	Overall survival			Disease-free survival		
			HR	95% CI	P	HR	95% CI	P
CEA ⩾ 3.4 ng/ml	23	38.3	1.514	0.704–3.257	0.289	1.883	0.969–3.658	0.062
Tumour size ⩾ 3.0 cm	26	43.3	1.283	0.663–2.484	0.460	1.179	0.641–2.170	0.596
Ly, moderate to severe	21	35.0	1.775	0.833–3.782	0.137	1.475	0.667–3.263	0.337
V, moderate to severe	19	31.7	2.178	1.059–4.479	0.034*	1.476	0.769–2.833	0.242
Peripheral CD204%^{high}	32	53.3	1.206	0.601–2.420	0.598	0.890	0.472–1.679	0.719
Plx-inv CD204%^{high}	20	33.3	2.624	1.242–5.544	0.011*	2.257	1.045–4.879	0.038*

* $P < 0.05$. Multivariate analysis was carried out using Cox regression model. HR, hazard ratio; 95% CI, 95% confidence interval; CEA, carcinoembryonic antigen; Ly, lymphatic invasion; V, vessel invasion; Peripheral CD204%^{high}, percentage of CD204-positive cells area at the periphery ⩾ 3.34; Plx-inv CD204%^{high}, percentage of CD204-positive cells area at extrapancreatic nerve plexus invasion ⩾ 0.57.

[31]. In our previous experimental study [12], neural invasion over a long distance could lead to severe neural damage. Additionally, the present study showed strong positive correlations among ne, plx-inv, long plx-inv distance and plx-inv CD204%^{high}. Taken together with the paracrine regulation between macrophages and tumour cells at plx-inv [14,15], severe neural invasion of tumour cells appears to recruit M2 macrophages due to neural damage. Moreover, the neural system was suggested as an expedient structure for interaction between tumour cells and M2 macrophages that promotes pancreatic cancer cell proliferation.

Adjuvant chemotherapy after complete resection of pancreatic IDC has been established as the definitive standard of care within the last decade [24,32,33]. In the present study, plx-inv CD204%^{high} was the only independent prognostic factor for poor OS and DFS in the group of patients with adjuvant chemotherapy. According to recent reports, immunoregulatory cytokines such as interleukin-6 and prostaglandin E2, which are present in the tumour microenvironment, are associated with chemoresistance and tumour-induced differentiation of tumour-promoting M2 macrophages [34,35]. Additional therapy to suppress M2 macrophages might thus prove effective, particularly against cases with plx-inv and high accumulation of M2 macrophages. Depletion of macrophages by zoledronic acid has been reported to enhance the effects of sorafenib in an *in vivo* model of metastatic liver cancer [36]. A phase II randomised controlled study of tasquinimod (oral quinolone-3-carboxamide) for metastatic castrate-resistant prostate cancer patients prolonged progression-free survival and confirmed the pharmacological efficacy of this agent for inhibiting S100A9 [37], which is a protein expressed in inflammatory cells that induces the maturation of macrophages [38]. Therefore, anti-M2 macrophage therapy may have potential as an innovative treatment for pancreatic IDC.

Limitations of this study include the retrospective manner of the investigation. Adjuvant chemotherapy was performed in 60 patients and was an independent factor predictive of OS and DFS, but the indication was influenced by time trends, and some degree of selection bias might have been present. Although OS and DFS for our patient cohort were comparable with the other previous studies [24,32,33], further investigation in patients with standardised adjuvant chemotherapy is needed. Moreover, since only resectable pancreatic cancer was studied, it is unknown whether the results can be extrapolated to the much higher numbers of unresectable cases.

In conclusion, pancreatic cancer patients with high accumulation of CD204-positive cells at plx-inv who underwent curative resection showed a high incidence

of recurrence in the form of peritoneal dissemination and locoregional recurrence and shorter OS and DFS. The impact of CD204-positive cells at plx-inv on OS and DFS was maintained in the setting of adjuvant chemotherapy. Increased infiltration of M2 macrophages at plx-inv may represent an important finding for detecting patients with aggressive IDC of the pancreas.

Conflict of interest statement

None declared.

Acknowledgement

Supported by Grants-In-Aid for Cancer Research and for the Third-term Comprehensive 10-year Strategy for Cancer Control from the Ministry of Health, Labour and Welfare of Japan; JSPS KAKENHI Grant Number 22790624; the National Cancer Center Research and Development Fund (23-A-2b).

References

[1] Siegel R, Ward E, Brawley O, et al. Cancer statistics, 2011: the impact of eliminating socioeconomic and racial disparities on premature cancer deaths. CA Cancer J Clin 2011;61:212–36.
[2] Hernandez JM, Morton CA, Al-Saadi S, et al. The natural history of resected pancreatic cancer without adjuvant chemotherapy. Am Surg 2010;76:480–5.
[3] Mitsunaga S, Hasebe T, Kinoshita T, et al. Detail histologic analysis of nerve plexus invasion in invasive ductal carcinoma of the pancreas and its prognostic impact. Am J Surg Pathol 2007;31:1636–44.
[4] Nagakawa T, Mori K, Nakano T, et al. Perineural invasion of carcinoma of the pancreas and biliary tract. Br J Surg 1993;80:619–21.
[5] Nakao A, Harada A, Nonami T, et al. Clinical significance of carcinoma invasion of the extrapancreatic nerve plexus in pancreatic cancer. Pancreas 1996;12:357–61.
[6] Chatterjee D, Katz MH, Rashid A, et al. Perineural and intraneural invasion in posttherapy pancreaticoduodenectomy specimens predicts poor prognosis in patients with pancreatic ductal adenocarcinoma. Am J Surg Pathol 2012;36:409–17.
[7] Takahashi H, Ohigashi H, Ishikawa O, et al. Perineural invasion and lymph node involvement as indicators of surgical outcome and pattern of recurrence in the setting of preoperative gemcitabine-based chemoradiation therapy for resectable pancreatic cancer. Ann Surg 2012;255:95–102.
[8] Tempero MA, Arnoletti JP, Behrman SW, et al. National Comprehensive Cancer Networks. Pancreatic Adenocarcinoma, version 2.2012: featured updates to the NCCN Guidelines. J Natl Compr Cancer Networks 2012;10:703–13.
[9] Imoto A, Mitsunaga S, Inagaki M, et al. Neural invasion induces cachexia via astrocytic activation of neural route in pancreatic cancer. Int J Cancer 2012;131:2795–807.
[10] Takahashi S, Hasebe T, Oda T, et al. Extra-tumor perineural invasion predicts postoperative development of peritoneal dissemination in pancreatic ductal adenocarcinoma. Anticancer Res 2001;21:1407–12.
[11] Zhu Z, Friess H, diMola FF, et al. Nerve growth factor expression correlates with perineural invasion and pain in human pancreatic cancer. J Clin Oncol 1999;17:2419–28.
[12] Mitsunaga S, Fujii S, Ishii G, et al. Nerve invasion distance is dependent on laminin gamma2 in tumors of pancreatic cancer. Int J Cancer 2010;127:805–19.
[13] Dai H, Li R, Wheeler T, et al. Enhanced survival in perineural invasion of pancreatic cancer: an in vitro approach. Hum Pathol 2007;38:299–307.
[14] Gil Z, Cavel O, Kelly K, et al. Paracrine regulation of pancreatic cancer cell invasion by peripheral nerves. J Natl Cancer Inst 2010;102:107–18.
[15] Cavel O, Shomron O, Shabtay A, et al. Endoneurial macrophages induce perineural invasion of pancreatic cancer cells by secretion of GDNF and activation of RET tyrosine kinase receptor. Cancer Res 2012;72:5733–43.
[16] Spilsbury K, O'Mara MA, Wu WM, et al. Isolation of a novel macrophage-specific gene by differential cDNA analysis. Blood 1995;85:1620–9.
[17] Ripoll VM, Irvine KM, Ravasi T, et al. Gpnmb is induced in macrophages by IFN-gamma and lipopolysaccharide and acts as a feedback regulator of proinflammatory responses. J Immunol 2007;178:6557–66.
[18] Mantovani A, Sozzani S, Locati M, et al. Macrophage polarization: tumor-associated macrophages as a paradigm for polarized M2 mononuclear phagocytes. Trends Immunol 2002;23:549–55.
[19] Ryder M, Ghossein RA, Ricarte-Filho JC, et al. Increased density of tumor-associated macrophages is associated with decreased survival in advanced thyroid cancer. Endocr Relat Cancer 2008;15:1069–74.
[20] Lissbrant IF, Stattin P, Wikstrom P, et al. Tumor associated macrophages in human prostate cancer: relation to clinicopathological variables and survival. Int J Oncol 2000;17:445–51.
[21] Ma YY, He XJ, Wang HJ, et al. Interaction of coagulation factors and tumor-associated macrophages mediates migration and invasion of gastric cancer. Cancer Sci 2011;102:336–42.
[22] Subimerb C, Pinlaor S, Khuntikeo N, et al. Tissue invasive macrophage density is correlated with prognosis in cholangiocarcinoma. Mol Med Report 2010;3:597–605.
[23] Yoshikawa K, Mitsunaga S, Kinoshita T, et al. Impact of tumor-associated macrophages on invasive ductal carcinoma of the pancreas head. Cancer Sci 2012;103:2012–20.
[24] Ueno H, Kosuge T, Matsuyama Y, et al. A randomised phase III trial comparing gemcitabine with surgery-only in patients with resected pancreatic cancer: Japanese Study Group of Adjuvant Therapy for Pancreatic Cancer. Br J Cancer 2009;101:908–15.
[25] Japan Pancreas Society. Classification of pancreatic carcinoma. 6th ed. Tokyo: Kanehara; 2009.
[26] Sobin LH, Gospodarowicz MK, Wittekind C. International union against cancer: TNM classification of malignant tumours. 7th ed. New York: Wiley-Blackwell; 2009.
[27] Fujino Y, Suzuki Y, Ajiki T, et al. Predicting factors for survival of patients with unresectable pancreatic cancer: a management guideline. Hepatogastroenterology 2003;50:250–3.
[28] Nakachi K, Furuse J, Ishii H, et al. Prognostic factors in patients with gemcitabine-refractory pancreatic cancer. Jpn J Clin Oncol 2007;37:114–20.
[29] Morizane C, Okusaka T, Morita S, et al. Construction and validation of a prognostic index for patients with metastatic pancreatic adenocarcinoma. Pancreas 2011;40:415–21.
[30] Rotshenker S. Wallerian degeneration: the innate-immune response to traumatic nerve injury. J Neuroinflammation 2011;8:109.
[31] Ceyhan GO, Bergmann F, Kadihasanoglu M, et al. Pancreatic neuropathy and neuropathic pain–a comprehensive pathomorphological study of 546 cases. Gastroenterology 2009;136:177–86.
[32] Neoptolemos JP, Stocken DD, Friess H, et al. A randomized trial of chemoradiotherapy and chemotherapy after resection of pancreatic cancer. N Engl J Med 2004;350:1200–10.
[33] Oettle H, Post S, Neuhaus P, et al. Adjuvant chemotherapy with gemcitabine vs observation in patients undergoing curative-intent

resection of pancreatic cancer: a randomized controlled trial. JAMA 2007;297:267–77.

[34] Dijkgraaf EM, Heusinkveld M, Tummers B, et al. Chemotherapy alters monocyte differentiation to favor generation of cancer-supporting M2 macrophages in the tumor microenvironment. Cancer Res 2013;73:2480–92.

[35] Zitvogel L, Apetoh L, Ghiringhelli F, Kroemer G. Immunological aspects of cancer chemotherapy. Nat Rev Immunol 2008; 8(1):59–73.

[36] Zhang W, Zhu XD, Sun HC, et al. Depletion of tumor-associated macrophages enhances the effect of sorafenib in metastatic liver cancer models by antimetastatic and antiangiogenic effects. Clin Cancer Res 2010;16:3420–30.

[37] Pili R, Häggman M, Stadler WM, et al. Phase II randomized, double-blind, placebo-controlled study of tasquinimod in men with minimally symptomatic metastatic castrate-resistant prostate cancer. J Clin Oncol 2011;29:4022–8.

[38] Sinha P, Okoro C, Foell D, et al. Proinflammatory S100 proteins regulate the accumulation of myeloid-derived suppressor cells. J Immunol 2008;181:4666–75.

What is the nature of pancreatic consistency? Assessment of the elastic modulus of the pancreas and comparison with tactile sensation, histology, and occurrence of postoperative pancreatic fistula after pancreaticoduodenectomy

Motokazu Sugimoto, MD, PhD,[a,b] Shinichiro Takahashi, MD, PhD,[a] Motohiro Kojima, MD, PhD,[b] Naoto Gotohda, MD, PhD,[a] Yuichiro Kato, MD,[a] Shingo Kawano, MD,[b] Atsushi Ochiai, MD, PhD,[b] *and* **Masaru Konishi, MD,[a]** *Chiba, Japan*

Background. *Although pancreatic consistency is a factor known to have an impact on the occurrence of postoperative pancreatic fistula (POPF) after pancreaticoduodenectomy (PD), it usually is assessed subjectively by the surgeon. Measurement of the elastic modulus (EM), a parameter characterizing the elasticity of a material, may be one approach for achieving objective and quantitative assessment of pancreatic consistency. This study was conducted to investigate the utility of determining the EM of the pancreas.*
Methods. *Fifty-nine patients who underwent PD and measurement of the EM of the ex vivo pancreas were investigated. Data for EM were compared with the tactile evaluation made by surgeons, histologic findings, and the occurrence of POPF.*
Results. *The EM of the pancreas was correlated with the tactile evaluation made by the surgeon (soft pancreas, 1.4 ± 2.1 kPa vs hard pancreas, 4.4 ± 5.1 kPa;* $P < .001$*). An EM of > 3.0 kPa was correlated with histologic findings including increased ratios of azan-Mallory positivity (*$P = .003$*) and α-smooth muscle actin positivity (*$P = .006$*), a decreased lobular ratio (*$P = .021$*), and an increased vessel density (*$P < .001$*). Patients with a pancreatic EM of < 3.0 kPa had an increased risk of POPF (hazard ratio, 9.333;* $P = .002$*).*
Conclusion. *Assessment of the EM of the resected pancreas reflects the tactile evaluation made by the surgeon and histological degree of pancreatic fibrosis, and is correlated with the occurrence of POPF after PD. (Surgery 2014;156:1204-11.)*

From the Department of Hepatobiliary-Pancreatic Surgery[a] and Division of Pathology,[b] Research Center for Innovative Oncology, National Cancer Center Hospital East, Kashiwa, Chiba, Japan

THE CONSISTENCY OF THE PANCREAS is a factor known to have an impact on the occurrence of postoperative pancreatic fistula (POPF) after pancreatic resection. In relation to pancreaticoduodenectomy (PD), it is accepted among pancreatic surgeons that in comparison with a "hard" pancreatic consistency, a "soft" consistency is associated with a greater incidence of POPF.[1-5] Pancreatic consistency usually is evaluated intraoperatively on the basis of the tactile sensation felt by surgeons and is thus a subjective and qualitative assessment.

The elastic modulus (EM) is a physical parameter[6] that characterizes the elasticity of a material. It

Supported in part by Health and Labour Sciences Research Grants for the Third Term Comprehensive Control Research for Cancer from the Ministry of Health, Labour and Welfare of Japan.

Accepted for publication May 16, 2014.

Reprint requests: Shinichiro Takahashi, MD, PhD, National Cancer Center Hospital East, 6-5-1 Kashiwa-no-ha, Kashiwa, Chiba 277-8577, Japan. E-mail: shtakaha@east.ncc.go.jp.

0039-6060/$ - see front matter

http://dx.doi.org/10.1016/j.surg.2014.05.015

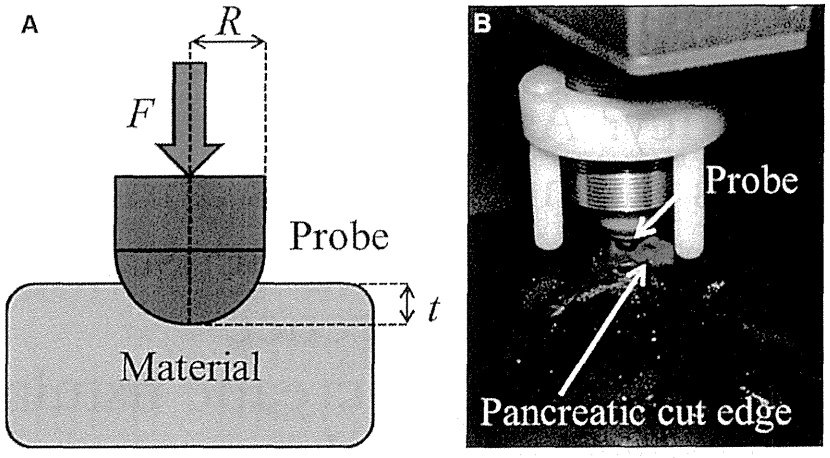

Fig 1. (*A*) Elastic material is indented vertically by a rigid spherical indenter probe. The elastic modulus (EM) of the material is calculated based on the contact stress theory of Hertz. *F*, Force exerted on an object under tension; *t*, variant of compression; *R*, radius of the spherical indenter probe. (*B*) Pancreatic cut surface (shown in *orange*) was indented vertically by a rigid spherical probe and released at a constant computer-controlled velocity. EM of the pancreas at an arbitrary indentation depth was calculated automatically. This procedure was performed using a Venustron apparatus.

has been applied for direct measurement of the elasticity of human tissues such as skin, bone, breast, and brain.[7-13] Different organs have a wide range of elasticity, and the elasticity of a specific organ may be altered as a result of various disease processes. For instance, Samani et al[12] reported that the mean EM of normal breast tissue was 1.9 kPa, that of fibroadenoma was 11.42 kPa, and that of invasive ductal carcinoma was 22.55 kPa.

With recent advances in diagnostic radiology, ultrasound elastography of the pancreas via the use of a transcutaneous or endoscopic approach has been reported increasingly for differential diagnosis of focal pancreatic lesions and pancreatic fibrosis.[14-19] Analyses that use endoscopic ultrasound elastography have demonstrated that the elastic parameters of the pancreatic parenchyma calculated by setting the surrounding soft tissue as a control are correlated with the degree of fibrotic change in the resected specimen.[14] The technique of elastography has now made it possible to evaluate a region of interest both qualitatively and quantitatively by monitoring the localized tissue displacement resulting from short-duration acoustic excitation to derive information on elasticity.[15]

To our knowledge, however, the feasibility of direct measurement of the EM of pancreatic tissue has never been evaluated. Comparison between the EM and the histologic characteristics of the pancreas may allow a better understanding of pathologic alterations of the pancreatic parenchyma, which may affect the consistency of the pancreas. Moreover, objective and quantitative evaluation of the EM of the pancreatic parenchyma might become a more widely acceptable means of assessing the risk of POPF after PD than is the case for subjective and qualitative assessment by the surgeon. The aim of the present study was to investigate the utility of assessment of the EM of the pancreas by evaluating its correlation with tactile sensation, histological findings, and the occurrence of POPF after PD.

METHODS

Patients and clinical data collection. Between November 2011 and May 2013, 59 PD specimens were used for ex vivo measurement of the EM of resected pancreas at the National Cancer Center Hospital East. The cut edge of the resected pancreas was evaluated histopathologically in all specimens to determine whether a sufficient operative margin for exclusion of tumor cells had been secured. Clinicopathologic data were reviewed from the medical records. During this period, the method used for reconstruction of the remnant pancreas and postoperative management were standardized. The study was approved by the institutional review board of the National Cancer Center (2012-067).

Operative techniques and perioperative management. Details of the operative maneuvers and perioperative management were described in our previous paper.[20] To summarize, subtotal stomach-preserving PD with D2 lymphadenectomy and modified Child's reconstruction were performed in all cases. End-to-side pancreaticojejunostomy was performed as a two-layered anastomosis with

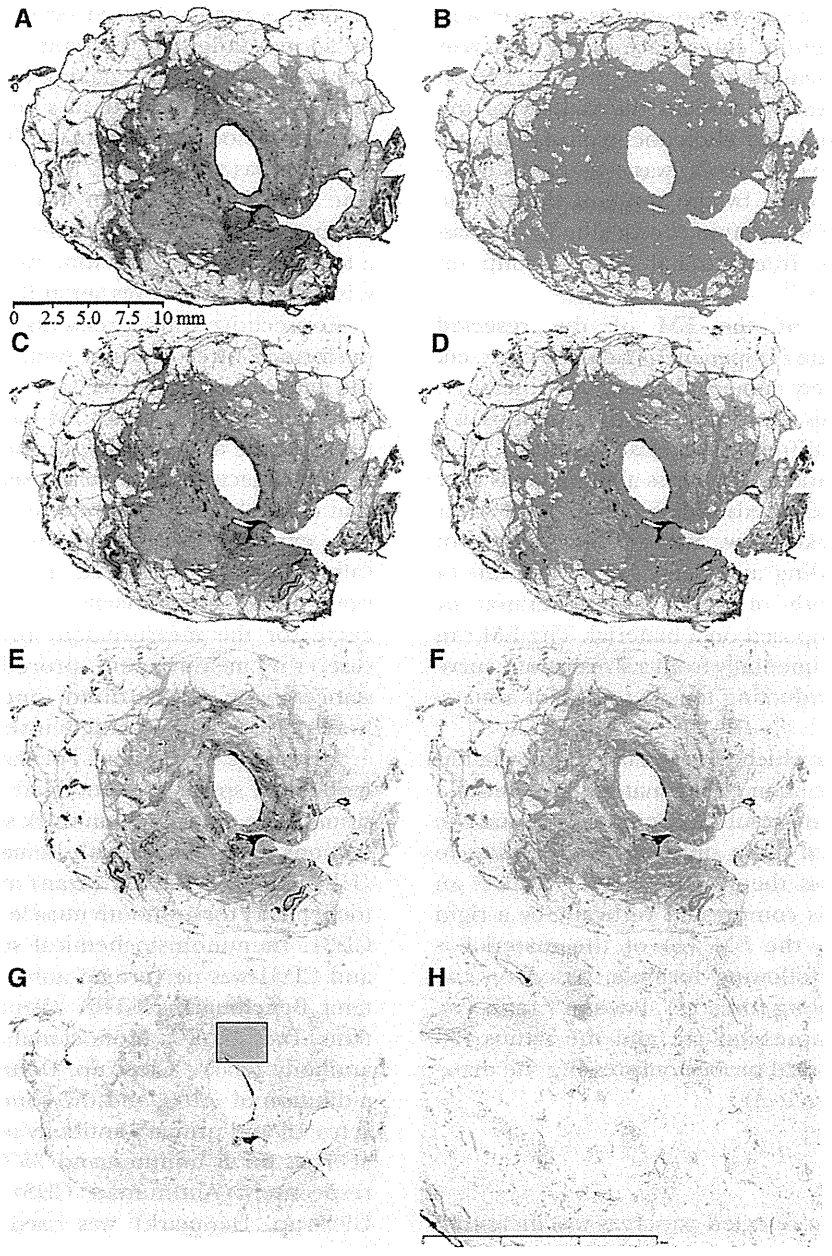

Fig 2. Histologic evaluation of the pancreatic stump. In this case, the EM of the pancreas was 13.0 kPa and the patient did not develop postoperative pancreatic fistula (POPF). (*A*) Loupe image of hematoxylin and eosin (HE)-stained slide. The outer circumference of the entire cut surface (*red line*) and the inner circumference of the main pancreatic duct (MPD) lumen (*blue line*) were automatically outlined, and these areas were calculated using the tracing algorithm of the WinROOF version 6.5 software (Mitani Corporation, Tokyo, Japan). The area of an entire cut surface (within the *red line*) was 367.0 mm^2, and the MPD area (within the *blue line*) was 10.59 mm^2. The MPD ratio was 2.89%, calculated as the percentage area of MPD in the entire cut surface. (*B*) The HE-positive area was determined as the visualized area stained with HE using the color-detecting algorithm of the software and identified as *bright green* in this image. The area of fat was defined as the area of an entire cut surface minus the MPD area and the HE-positive area. The fat ratio was 37.5%, calculated as the percentage area of fat in an entire cut surface. (*C*) Azan-Mallory (azan) staining was evaluated on the loupe image to determine the degree of fibrosis. (*D*) The azan-positive area was determined as the visualized area stained with aniline blue using the color-detecting algorithm of the software, and identified as *bright green* in this image. The azan-positive ratio was 24.8%, calculated as the percentage area of azan positivity in an entire cut surface. The lobular area was defined as the HE-positive area minus the MPD area and the azan-positive area. The lobular ratio was 34.8%, calculated as the percentage area of lobules in an entire cut surface. (*E*) Loupe image of